

Tracking of Multiple Moving Sources Using Recursive EM Algorithm

Pei–Jung Chung*, Johann F. Böhme**, Alfred O. Hero*

* Dept. of Electrical Engineering and Computer Science, University of Michigan, Ann Arbor, USA

** Signal Theory Group, Dept. of Electrical Engineering and Information Science

Ruhr-Universität Bochum, D-44780 Bochum, Germany

Email: peijung_chung@yahoo.com, boehme@sth.ruhr-uni-bochum.de, hero@eecs.umich.edu

Abstract

This work deals with recursive direction of arrival (DOA) estimation of multiple moving sources. Based on the recursive EM algorithm, we develop two recursive procedures to estimate the time-varying DOA parameter for narrow band signals. The first procedure requires no prior knowledge about the source movement. The second procedure assumes that the motion of moving sources is described by a linear polynomial model. The proposed recursion updates the polynomial coefficients when a new data arrives. The suggested approaches have two major advantages: simple implementation and easy extension to wideband signals. Numerical experiments show that both procedures provide excellent results in a slowly changing environment. When the DOA parameter changes fast or two source directions cross with each other, the procedure designed for a linear polynomial model has a better performance than the general procedure. Compared to the beamforming technique [17] based on the same parameterization, our approach is computationally favorable and has a wider range of applications.

1 Introduction

The problem of estimating direction of arrival (DOA) of plane waves impinging on a sensor array is of fundamental importance in many applications such as radar, sonar, geophysics and wireless communication. The maximum likelihood (ML) method is known to have excellent statistical performance and is robust against coherent signals and small sample numbers [2]. However, the high computational cost associated with ML method makes it less attractive in practice.

To improve the computational efficiency of the ML approach, numerical methods such as the expectation and maximization (EM) algorithm [11] was suggested in [12] [5][16]. Recursive procedures based on the recursive EM algorithm for estimating constant DOA parameters were discussed in [6] [15]. Similar procedures for tracking multiple moving sources were studied in [8] [13]. In [13], the authors focused on narrow band sources and assumed known signal waveforms.

The recursive EM algorithm is a stochastic approximation procedure for finding ML estimates. It was first suggested by Titterton [18] and extended to the multi-dimensional case in [6]. As it was pointed out by Titterton, recursive EM can be seen as a sequential approximation of the EM algorithm. The gain matrix of recursive EM is the inversion of the augmented data information matrix. Through proper design of the augmentation scheme, the augmented data and the corresponding information matrix usually have a simple structure [11]. In this case, the recursive EM algorithm is very easy to implement. For constant parameter, estimates generated by recursive EM are strongly consistent and asymptotically normally distributed. For time-varying parameter, the tracking ability of a stochastic approximation procedure depends mainly on the dynamics of the true parameter, gain matrix and step size [1].

Based on recursive EM, we shall derive two recursive procedures for estimating time-varying DOA. The first procedure does not require any prior knowledge on the motion model. The only assumption is that the unknown parameter changes slowly with time. The second procedure assumes that the time-varying DOA parameter $\theta(t)$ is described by a linear polynomial of time. This model is important since a smooth function $\theta(t)$ can be approximated by a local linear polynomial in a short time interval [17]. The procedure reported in [8] employs a decreasing step size to estimate the polynomial coefficients. However, since the DOA parameter $\theta(t)$ and the log-likelihood function change with time, a decreasing step size may not capture the non-stationary feature of the underlying system over a long period. To overcome this problem, we suggest a constant step size to be used in the algorithm. It is noteworthy that both procedures

are aimed at maximizing the expected concentrated likelihood function [9]. Introducing a linear polynomial model implies increasing the dimension of the parameter space. With the additional degree of freedom, the procedure designed for a linear polynomial model should perform better than the general one.

In contrast to methods based on subspace tracking [22] or two dimensional beamforming [17], our approach can be easily generalized to wideband cases including underwater acoustic signals. Unlike the Kalman type algorithms [23], recursive procedures considered here have a much simpler implementation.

This paper is outlined as follows. We describe the signal model and the recursive EM algorithm briefly in section 2 and section 3. Section 4 presents two recursive procedures for localizing moving sources. Simulation results are discussed in section 5. We give concluding remarks in section 6.

2 Problem Formulation

Consider an array of N sensors receiving M far field waves from unknown time-varying directions $\boldsymbol{\theta}(t) = [\theta_1(t) \dots \theta_M(t)]$. The array output $\mathbf{x}(t) \in \mathbb{C}^{N \times 1}$ at time instant t is expressed as

$$\mathbf{x}(t) = \mathbf{H}(\boldsymbol{\theta}(t))\mathbf{s}(t) + \mathbf{u}(t), \quad t = 1, 2, \dots \quad (1)$$

where the steering matrix

$$\mathbf{H}(\boldsymbol{\theta}(t)) = [\mathbf{d}(\theta_1(t)) \dots \mathbf{d}(\theta_M(t))] \in \mathbb{C}^{N \times M} \quad (2)$$

consists of M steering vectors $\mathbf{d}(\theta_m(t)) \in \mathbb{C}^{N \times 1}$, ($m = 1, \dots, M$). To avoid ambiguity, we assume $M < N$. The signal waveform $\mathbf{s}(t) = [s_1(t) \dots s_M(t)]^T \in \mathbb{C}^{M \times 1}$ is considered as unknown and deterministic. $(\cdot)^T$ denotes the transpose of a vector. Furthermore, the noise process $\mathbf{u}(t) \in \mathbb{C}^{N \times 1}$ is independent identically complex normally distributed with zero mean and covariance matrix $\nu \mathbf{I}$, where ν represents the unknown noise spectral parameter and \mathbf{I} is the identity matrix.

In the following, we assume that the number of sources M is known. Standard procedures based on MDL criterion [20] or multiple hypothesis testing [15] can be used to determine M . The problem of interest is to estimate the time-varying DOA parameter $\boldsymbol{\theta}(t)$ recursively from the observation $\mathbf{x}(t)$. We assume that a good initial estimate $\boldsymbol{\theta}^0$ is available at the beginning of the recursion.

3 Recursive Parameter Estimation Using Incomplete Data

The recursive EM algorithm suggested by Titterton is a stochastic approximation procedure for finding maximum likelihood estimates (MLE). As pointed out in [18], there is a strong relationship between this procedure and the EM algorithm [11]. Using Taylor expansion, Titterton showed that approximately, recursive EM maximizes EM's augmented log-likelihood sequentially. The unknown parameter is considered as constant in [18]. In the fixed parameter case, a properly chosen decreasing step size is necessary to ensure strong consistency and asymptotic normality of the algorithm [7] [18].

Suppose $\mathbf{x}(1), \mathbf{x}(2), \dots$ are independent observations, each with underlying probability density function (pdf) $f(\mathbf{x}; \boldsymbol{\vartheta})$, where $\boldsymbol{\vartheta}$ denotes an unknown constant parameter. The augmented data associated with EM $\mathbf{y}(1), \mathbf{y}(2), \dots$ are characterized by the pdf $f(\mathbf{y}; \boldsymbol{\vartheta})$. According to [11], the augmented data $\mathbf{y}(t)$ is so specified that $\mathcal{M}(\mathbf{y}(t)) = \mathbf{x}(t)$ is a many-to-one mapping. Let $\boldsymbol{\vartheta}^t$ denote the estimate after t observations. The following procedure is aimed at finding the true parameter $\boldsymbol{\vartheta}$ which may coincide with the MLE in the asymptotic sense [19]

$$\boldsymbol{\vartheta}^{t+1} = \boldsymbol{\vartheta}^t + \epsilon_t \mathcal{I}_{EM}(\boldsymbol{\vartheta}^t)^{-1} \boldsymbol{\gamma}(\mathbf{x}(t), \boldsymbol{\vartheta}^t) \quad (3)$$

where ϵ_t is a decreasing step size and

$$\mathcal{I}_{EM}(\boldsymbol{\vartheta}^t) = \text{E} \left[-\nabla_{\boldsymbol{\vartheta}} \nabla_{\boldsymbol{\vartheta}}^T \log f(\mathbf{y}; \boldsymbol{\vartheta}) \mid \mathbf{x}(t), \boldsymbol{\vartheta} \right]_{\boldsymbol{\vartheta}=\boldsymbol{\vartheta}^t}, \quad (4)$$

$$\boldsymbol{\gamma}(\mathbf{x}(t), \boldsymbol{\vartheta}^t) = \nabla_{\boldsymbol{\vartheta}} \log f(\mathbf{x}(t); \boldsymbol{\vartheta})|_{\boldsymbol{\vartheta}=\boldsymbol{\vartheta}^t} \quad (5)$$

represent the augmented information matrix and gradient vector, respectively. $\nabla_{\boldsymbol{\vartheta}}$ is a column gradient operator with respect to $\boldsymbol{\vartheta}$. We assume that both (4) and (5) exist. Under mild conditions, the estimates generated by (3) are strongly consistent and asymptotic normally distributed. In view of the well-known singularities and multiple maxima that are on likelihood surfaces, one could of course not expect consistency irrespective of the starting point [18].

The augmented data \mathbf{y} usually has a simpler structure than the observed data \mathbf{x} . Therefore, the augmented data information matrix $\mathcal{I}_{EM}(\boldsymbol{\vartheta}^t)$ is easier to compute and invert than the observed data information matrix $\mathcal{I}(\boldsymbol{\vartheta}^t) = \text{E} \left[-\nabla_{\boldsymbol{\vartheta}} \nabla_{\boldsymbol{\vartheta}}^T \log f(\mathbf{x}; \boldsymbol{\vartheta}) \mid \mathbf{x}(t), \boldsymbol{\vartheta} \right]_{\boldsymbol{\vartheta}=\boldsymbol{\vartheta}^t}$. Although recursive EM does not have the optimal convergence rate in the Cramér-Rao sense as the following

procedure [18]

$$\boldsymbol{\vartheta}^{t+1} = \boldsymbol{\vartheta}^t + \epsilon_t \mathcal{I}(\boldsymbol{\vartheta}^t)^{-1} \boldsymbol{\gamma}(\mathbf{x}(t), \boldsymbol{\vartheta}^t), \quad (6)$$

it is much easier to implement than (6). Using $\mathcal{I}_{EM}(\boldsymbol{\vartheta}^t)^{-1}$ as the gain matrix is a trade-off between convergence rate and computational cost.

When the parameter of interest varies with time, a decreasing step size such as $\epsilon_t = t^{-\alpha}$, $1/2 < \alpha \leq 1$ can not capture the non-stationary feature of the underlying system. A classical way to overcome this difficulty is to replace ϵ_t with a constant step size ϵ . In general, a large step size reduces the bias and increases the variance of the estimates [1]. A small step size has the opposite effects. Since the time varying parameter $\boldsymbol{\vartheta}(t)$ may follow a complicated dynamics, an exact investigation of the convergence behavior of the algorithm

$$\boldsymbol{\vartheta}^{t+1} = \boldsymbol{\vartheta}^t + \epsilon \mathcal{I}_{EM}(\boldsymbol{\vartheta}^t)^{-1} \boldsymbol{\gamma}(\mathbf{x}(t), \boldsymbol{\vartheta}^t) \quad (7)$$

is only possible when certain assumptions are made on the parameter model. More discussion about convergence properties of a stochastic approximation procedure in a non-stationary environment can be found in [1].

4 Localization of Moving Sources

The recursive EM algorithm with constant step size (7) is applied to estimate the time-varying DOA parameter $\boldsymbol{\theta}(t)$. We start with a general case in which $\boldsymbol{\theta}(t)$ changes slowly with time and then consider a linear polynomial model.

4.1 General Case

From the signal model in section 2, we know that the array observation $\mathbf{x}(t)$ is complex normally distributed with the the log-likelihood function

$$\log f(\mathbf{x}(t); \boldsymbol{\vartheta}) = - \left[N \log \pi + N \log \nu + \frac{1}{\nu} (\mathbf{x}(t) - \mathbf{H}(\boldsymbol{\theta}(t))\mathbf{s}(t))^H (\mathbf{x}(t) - \mathbf{H}(\boldsymbol{\theta}(t))\mathbf{s}(t)) \right] \quad (8)$$

where $\boldsymbol{\vartheta} = [\boldsymbol{\theta}(t)^T \mathbf{s}(t)^T \nu]^T$ and $(\cdot)^H$ denotes the Hermitian transpose.

According to (7), all elements in $\boldsymbol{\vartheta}$ should be updated simultaneously. Since we are mainly interested in the DOA parameter $\boldsymbol{\theta}(t)$ and including $\{\mathbf{s}(t), \nu\}$ in the recursion will complicate the gain matrix $\mathcal{I}_{EM}(\boldsymbol{\vartheta}^t)^{-1}$, the procedure (7) is only applied to $\boldsymbol{\theta}(t)$. The estimate for signal

waveform and noise level, denoted by $\mathbf{s}^t = [s_1^t \ s_2^t \ \dots \ s_M^t]^T$ and ν^t respectively, are updated by computing their ML estimates once the current DOA estimate is available. For simplicity, we use $\boldsymbol{\theta}$ instead of $\boldsymbol{\theta}(t)$ in the following discussion.

Taking the first derivative on the right hand side of (8) with respect to θ_m , we obtain the m th element of the gradient vector $\boldsymbol{\gamma}(\mathbf{x}(t), \boldsymbol{\vartheta}^t)$ [7]

$$[\boldsymbol{\gamma}(\mathbf{x}(t), \boldsymbol{\vartheta}^t)]_m = \frac{2}{\nu^t} \text{Re} [(\mathbf{x}(t) - \mathbf{H}(\boldsymbol{\theta}^t) \mathbf{s}^t)^H (\mathbf{d}'(\theta_m) s_m^t)], \quad (9)$$

where $\mathbf{d}'(\theta_m) = \partial \mathbf{d}(\theta_m) / \partial \theta_m$.

The augmented data $\mathbf{y}(t)$ is obtained by decomposing the array output into its signal and noise parts. Formally it is expressed as

$$\mathbf{y}(t) = [\mathbf{y}_1(t)^T \ \dots \ \mathbf{y}_m(t)^T \ \dots \ \mathbf{y}_M(t)^T]^T. \quad (10)$$

The augmented data associated with the m th signal

$$\mathbf{y}_m(t) = \mathbf{d}(\theta_m) s_m(t) + \mathbf{u}_m(t) \quad (11)$$

is complex normally distributed with mean $\mathbf{d}(\theta_m) s_m(t)$ and covariance matrix $\nu_m \mathbf{I}$ with the constraint $\sum_{m=1}^M \nu_m = \nu$. A convenient choice is $\nu_m = \nu/M$. The corresponding log-likelihood is given by

$$\log f(\mathbf{y}(t); \boldsymbol{\vartheta}) = - \sum_{m=1}^M \left[N \log \pi + N \log(\nu/M) + \frac{M}{\nu} (\mathbf{y}_m(t) - \mathbf{d}(\theta_m) s_m(t))^H (\mathbf{y}_m(t) - \mathbf{d}(\theta_m) s_m(t)) \right]. \quad (12)$$

Since the signals are decoupled through the augmentation scheme (10), $\mathcal{I}_{EM}(\boldsymbol{\vartheta}^t)$ is a $M \times M$ diagonal matrix when we only consider the DOA parameter $\boldsymbol{\theta}$. By definition (4), the m th diagonal element of $\mathcal{I}_{EM}(\boldsymbol{\vartheta}^t)$ is the conditional expectation of the second derivative of the augmented log-likelihood

$$[\mathcal{I}_{EM}(\boldsymbol{\vartheta}^t)]_{mm} = \mathbb{E} \left[- \frac{\partial^2}{\partial \theta_m^2} \log f(\mathbf{y}(t); \boldsymbol{\vartheta}) \mid \mathbf{x}(t), \boldsymbol{\vartheta}^t \right], \quad (13)$$

which is given by

$$[\mathcal{I}_{EM}(\boldsymbol{\vartheta}^t)]_{mm} = \frac{2}{\nu^t} \text{Re} \left[- (\mathbf{d}''(\theta_m) s_m^t)^H (\mathbf{x}(t) - \mathbf{H}(\boldsymbol{\theta}^t) \mathbf{s}^t) + M \|\mathbf{d}'(\theta_m) s_m^t\|^2 \right] \quad (14)$$

where $\mathbf{d}''(\theta_m) = \partial^2 \mathbf{d}(\theta_m) / \partial \theta_m^2$.

Once the estimate $\boldsymbol{\theta}^{t+1}$ is available, the signal and noise parameters are obtained by computing their ML estimates at current $\boldsymbol{\theta}^{t+1}$ and $\mathbf{x}(t)$ as follows

$$\mathbf{s}^{t+1} = \mathbf{H}(\boldsymbol{\theta}^{t+1})^\# \mathbf{x}(t), \quad (15)$$

$$\nu^{t+1} = \frac{1}{N} \text{tr} \left[\mathbf{P}(\boldsymbol{\theta}^{t+1})^\perp \widehat{\mathbf{C}}_{\mathbf{x}}(t) \right], \quad (16)$$

where $\mathbf{H}(\boldsymbol{\theta}^{t+1})^\#$ is the generalized left inverse of the matrix $\mathbf{H}(\boldsymbol{\theta}^{t+1})$, $\mathbf{P}(\boldsymbol{\theta}^{t+1})^\perp = \mathbf{I} - \mathbf{P}(\boldsymbol{\theta}^{t+1})$ is the orthogonal complement of the projection matrix $\mathbf{P}(\boldsymbol{\theta}^{t+1}) = \mathbf{H}(\boldsymbol{\theta}^{t+1})\mathbf{H}(\boldsymbol{\theta}^{t+1})^\#$ and $\widehat{\mathbf{C}}_{\mathbf{x}}(t) = \mathbf{x}(t)\mathbf{x}(t)^H$.

Given a constant step size ϵ , the number of sources M and the current estimate $\boldsymbol{\theta}^t$, the $(t + 1)$ st recursion of the algorithm proceeds as follows.

<p>Recursive EM algorithm I (arbitrary motion)</p> <p>(1) Calculate gradient vector $\boldsymbol{\gamma}(\mathbf{x}(t), \boldsymbol{\theta}^t)$ by eq.(9) and the matrix $\mathcal{I}_{EM}(\boldsymbol{\theta}^t)$ by eq.(14).</p> <p>(2) Update DOA parameters by $\boldsymbol{\theta}^{t+1} = \boldsymbol{\theta}^t + \epsilon [\mathcal{I}_{EM}(\boldsymbol{\theta}^t)]^{-1} \boldsymbol{\gamma}(\mathbf{x}(t), \boldsymbol{\theta}^t).$</p> <p>(3) Update signal and noise parameter \mathbf{s}^t, ν^t by eqs.(15), (16).</p>
--

Table 1: Recursive EM algorithm I (REM I)

4.2 Linear Polynomial Model

We consider moving sources described by the linear polynomial model

$$\boldsymbol{\theta} = \boldsymbol{\theta}_0 + t \boldsymbol{\theta}_1, \quad (17)$$

where $\boldsymbol{\theta}_0 = [\theta_{01}, \dots, \theta_{0M}]^T$ and $\boldsymbol{\theta}_1 = [\theta_{11}, \dots, \theta_{1M}]^T$. The linear polynomial (17) can be seen as a truncated Taylor expansion which gives a good description for the source motion in a small observation interval [17].

The recursive EM algorithm is applied to estimate $\boldsymbol{\theta}_0$ and $\boldsymbol{\theta}_1$. For notational simplicity, we define the extended DOA parameter as $\boldsymbol{\Theta} = [\boldsymbol{\Theta}_1^T \dots \boldsymbol{\Theta}_m^T \dots \boldsymbol{\Theta}_M^T]^T$ where $\boldsymbol{\Theta}_m = [\theta_{0m}, \theta_{1m}]^T$.

Similarly to the procedure presented in subsection 4.1, recursive EM is only applied to update the DOA parameter Θ , rather than $\boldsymbol{\vartheta} = [\Theta^T \mathbf{s}(t)^T \nu]^T$.

Based on this approach, the $2m$ th and $(2m + 1)$ st element of the gradient vector $\boldsymbol{\gamma}(\mathbf{x}(t), \boldsymbol{\vartheta}^t)$ are given by

$$\frac{\partial}{\partial \theta_{0m}} \log f(\mathbf{x}(t); \boldsymbol{\vartheta})|_{\boldsymbol{\vartheta}=\boldsymbol{\vartheta}^t} = \frac{2}{\nu^t} \text{Re} [(\mathbf{x}(t) - \mathbf{H}(\Theta^t) \mathbf{s}^t)^H (\mathbf{d}'(\Theta_m^t) s_m^t)] \quad (18)$$

and

$$\frac{\partial}{\partial \theta_{1m}} \log f(\mathbf{x}(t); \boldsymbol{\vartheta})|_{\boldsymbol{\vartheta}=\boldsymbol{\vartheta}^t} = \frac{2t}{\nu^t} \text{Re} [(\mathbf{x}(t) - \mathbf{H}(\Theta^t) \mathbf{s}^t)^H (\mathbf{d}'(\Theta_m^t) s_m^t)], \quad (19)$$

respectively, where $\mathbf{d}'(\Theta_m^t) = \partial \mathbf{d}(\theta_m) / \partial \theta_m |_{\theta_m = \theta_{m0}^t + t \theta_{m1}^t}$. Note that θ is calculated at the current estimate Θ^t according to the linear model (17).

Because each source is described by two unknown parameters, the augmented data information matrix becomes block diagonal. Unfortunately, this matrix is singular under current parameterization. To avoid singularity and simplify the recursion, rather than using this block diagonal matrix in the recursion directly, we consider an alternative matrix $\tilde{\mathcal{I}}_{EM}(\boldsymbol{\vartheta}^t)$ which is the diagonal part of $\mathcal{I}_{EM}(\boldsymbol{\vartheta}^t)$.

Let $\mathbf{d}''(\Theta^t) = \partial^2 \mathbf{d}(\theta_m) / \partial \theta_m^2 |_{\theta_m = \theta_{m0}^t + t \theta_{m1}^t}$. According to the augmentation scheme specified above, the $2m$ th and $(2m + 1)$ st diagonal components of $\tilde{\mathcal{I}}_{EM}(\Theta^t)$ are given by

$$\frac{2}{\nu^t} \text{Re} \left[(-\mathbf{d}''(\Theta_m^t) s_m^t)^H (\mathbf{x}(t) - \mathbf{H}(\Theta^t) s_m^t) + M \|\mathbf{d}'(\Theta_m^t) s_m^t\|^2 \right] \quad (20)$$

and

$$\frac{2t^2}{\nu^t} \text{Re} \left[(-\mathbf{d}''(\Theta_m^t) s_m^t)^H (\mathbf{x}(t) - \mathbf{H}(\Theta^t) s_m^t) + M \|\mathbf{d}'(\Theta_m^t) s_m^t\|^2 \right], \quad (21)$$

respectively.

Similarly to the general case, the signal and noise parameter are updated by (15) and (16) once the estimate Θ^{t+1} is available. The parameter θ^{t+1} in (15) and (16) is replaced by Θ^{t+1} .

Given the step size ϵ , the number of sources M and the current estimate Θ^t , the $(t + 1)$ st recursion of the algorithm proceeds as follows.

<p>Recursive EM algorithm II (linear polynomial model)</p> <p>(1) Calculate gradient vector $\gamma(\mathbf{x}(t), \Theta^t)$ by eqs.(18), (19) and the matrix $\tilde{\mathcal{I}}_{EM}(\Theta^t)$ by eqs.(20),(21).</p> <p>(2) Update DOA parameters by $\Theta^{t+1} = \Theta^t + \epsilon [\tilde{\mathcal{I}}_{EM}(\Theta^t)]^{-1} \gamma(\mathbf{x}(t), \Theta^t)$.</p> <p>(3) Update signal and noise parameter s^t, ν^t by eqs.(15), (16). with θ^t replaced by Θ^t.</p>

Table 2: Recursive EM algorithm II (REM II)

For simplicity, the recursive EM for the general case and the recursive EM for the linear polynomial model are referred to as “REM I” and “REM II”, respectively.

From eqs. (9), (14), (15) and (16), the computational complexity of REM I lies approximately between $O(MN + MN^2)$ and $O(MN + N^3)$. The dominant term MN^2 (or N^3) is associated with s^{t+1} given by (15) which is a solution to a least square (LS) problem. Different LS algorithms yield different computational loads [14]. Due to the increased number of unknowns, REM II requires twice as many computations as REM I in computing the gradient vector and augmented information matrix. Clearly, REM II is computationally more efficient than the local polynomial approximation based beamforming technique [17] whose computational complexity is given by $O(NTLP)$ where T represents the number of snapshots, L denotes the number of points in the angular search domain and P denotes the number of angular velocity search domain.

It was pointed out in [9] that recursive EM for constant DOA estimation is indeed a recursive procedure for finding the maximum of the expected concentrated likelihood function

$$\mathcal{L}(\theta) = -\text{tr} \log [\mathbf{P}(\theta) \mathbf{C}_{\mathbf{x}}(t)] \quad (22)$$

where $\mathbf{C}_{\mathbf{x}}(t) = \mathbf{E} [\mathbf{x}(t) \mathbf{x}(t)^H]$. The constant step size considered in REM I captures the time-varying character of the likelihood function. Similarly, REM II is aimed at finding the maximum of $\mathcal{L}(\theta)$. Using a different parameterization such as a linear polynomial model implies increasing the dimension of the parameter space. With the additional degree of freedom, REM II is expected to have a better tracking ability. Later in section 5 we shall show that in critical situations where

two source directions cross with each other, recursive EM algorithm II provides more accurate estimates than REM I.

Choosing a proper step size plays an important role in the algorithms' tracking ability. The optimal step size depends on the dynamics of the true parameters, for instance, rate of change. Interested readers can find general guidelines in [1] and an adaptive procedure designed for recursive EM with decreasing step size in [10].

4.3 Extension to Broadband Signals

The algorithms presented previously are derived under the narrow band signal assumption. Extension to the broadband case is straightforward. From the asymptotic theory of Fourier transform [4], we know that each frequency bin is asymptotically independent from each other [3]. The log-likelihood function associated with the broadband signal is a sum of the log-likelihoods of individual frequency bins. Correspondingly, the gradient vector and augmented information matrix can be easily obtained by adding up the gradient vectors and augmented data information matrices of relevant frequency bins. Similarly to the narrow band case, the signal and noise parameters at each frequency are updated by calculating their ML estimates once the current DOA estimate is available.

5 Simulation

The proposed algorithms are tested by numerical experiments. In the first part, we consider recursive EM algorithms' application in narrow band and broadband cases. In the second part, we compare REM II with the local polynomial approximation (LPA) based beamforming technique [17].

5.1 Recursive EM algorithms I and II

The narrow band signals generated by three sources of equal power are received by a uniformly linear array of 15 sensors with inter-element spacings of half a wavelength. The Signal to Noise Ratio (SNR), defined as $10 \log(s_m(t)^2/\nu)$, $m = 1, 2, 3$, is kept at 10, 20 dB. The motion of the moving sources is described by a linear polynomial model

$$\boldsymbol{\theta} = \boldsymbol{\theta}_0 + t \boldsymbol{\theta}_1 \quad (23)$$

Three different parameter sets $\{\boldsymbol{\theta}_0, \boldsymbol{\theta}_1\}$ are assumed in the experiments. Each experiment performs 200 trials.

In the first experiment, we consider relatively fast moving sources. The true parameters are given by $\boldsymbol{\theta}_0 = [10^\circ, 60^\circ, 66^\circ]$, $\boldsymbol{\theta}_1 = [0.6^\circ, -1.0^\circ, 0.4^\circ]$ where $\boldsymbol{\theta}_1$ is measured by degree per time unit. In order to get a good insight into the tracking behavior, the same initial values are used in all trials. We applied LPA based beamforming to 20 snapshots to obtain the initial estimates $\boldsymbol{\theta}_0^0 = [10.5^\circ, 59.5^\circ, 68.5^\circ]$, $\boldsymbol{\theta}_1^0 = [0.58^\circ, -0.99^\circ, 0.38^\circ]$. The initial estimate for REM I is given by $\boldsymbol{\theta}_0^0$. Both algorithms use a constant step size $\epsilon = 0.6$. Figs. 1 and 2 present the true values of $\boldsymbol{\theta}$ and an example of estimated trajectories. As shown in both figures, two source directions cross with each other at $t = 32$. Obviously, the recursive procedure designed for the most general case can not follow fast moving sources at all. In contrast, the estimated trajectory obtained by REM II is very close to the true one. Figs. 3 and 4 show the mean square errors (RMSE) of the DOA estimates, defined as $\sqrt{\|\boldsymbol{\theta}^t - \boldsymbol{\theta}\|^2}$, averaged over 200 trials. Since REM I fails to track the moving sources, the corresponding RMSE grows with increasing time. On the other hand, the RMSE associated with REM II decreases slightly at the beginning of the recursion and then remains almost constant. Comparing Figs. 3 and 4, one can observe that SNR= 20 dB has a slightly lower RMSE than SNR= 10 dB.

The second experiment involves three slowly moving sources. The true parameter values are given by $\boldsymbol{\theta}_0 = [30^\circ, 50^\circ, 62^\circ]$, $\boldsymbol{\theta}_1 = [0.06^\circ, -0.1^\circ, 0.05^\circ]$. Note that the angular velocity $\boldsymbol{\theta}_1$ is approximately 1/10 of that considered in the previous experiment. We applied the ML method to obtain the initial estimates $\boldsymbol{\theta}_0^0 = [30.1^\circ, 50.8^\circ, 60.9^\circ]$. Because the angular velocity is very small compared to that in the previous experiment, we take $\boldsymbol{\theta}_1^0 = [0^\circ, 0^\circ, 0^\circ]$ as the initial value for $\boldsymbol{\theta}_1$. The initial estimate for REM I is given by $\boldsymbol{\theta}_0^0$. Both algorithms use a constant step size $\epsilon = 0.6$. Figs. 5 and 6 present the true and estimated trajectories obtained by REM I and REM II. Similarly to the first experiment, two source directions cross with each other at $t = 126$. The estimated trajectory by REM I is close to the true one when no crossing happens. Between $t = 100$ and $t = 230$ where two source directions cross with each other, the estimated trajectories associated with the first two sources do not get close to each other. Instead, they just depart in the vicinity of $t = 126$. For the same scenario, REM II provides a more accurate estimate. Fig. 6 shows that the crossing point causes a larger deviation from the true trajectory. Due to a higher sensitivity to the variation of angular velocity at the crossing point, the estimated trajectory in

fig. 6 is slightly worse than that in fig. 2. Comparison of figs. 7 and 8 with figs. 3 and 4, shows an overall lower RMSE in this scenario. Although REM I provides more reliable estimates than in the first experiment, REM II still outperforms REM I.

In the third experiment, three sources move slowly with different speeds but do not cross with each other. The true parameters are given by $\boldsymbol{\theta}_0 = [10^\circ, 30^\circ, 62^\circ]$, $\boldsymbol{\theta}_1 = [0.08^\circ, 0.1^\circ, 0.06^\circ]$. The initial estimates are $\boldsymbol{\theta}_0^0 = [10.04^\circ, 30.04^\circ, 62.05^\circ]$, $\boldsymbol{\theta}_1^0 = [0^\circ, 0^\circ, 0^\circ]$. We use a constant step size $\epsilon = 0.6$. Both algorithms have good tracking ability. Figs. 9 and 10, show that RMSE is the lowest among all three scenarios. REM II has a better performance than REM I. While REM II has a better performance at higher SNR, REM I seems to be less sensitive to SNRs in all three scenarios.

In addition to the narrow band signals, we also applied REM I and II to broadband signals with 3 frequency bins. The scenario similar to the second experiment leads to results presented in figs. 11 to 12. The estimates behave similar to the narrow band case. Comparison of RMSEs shows that more frequency bins leads to higher accuracy.

5.2 Comparison with LPA beamforming

We compare REM II with the LPA based beamforming approach suggested by Katkovnik and Gershman [17]. Both algorithms assume the motion model (17). In the first experiment, the narrow band signals are generated by the following parameter set $\boldsymbol{\theta}_0 = [10^\circ, 60^\circ]$, $\boldsymbol{\theta}_1 = [0.6^\circ, -1.0^\circ]$, SNR= 0, 10 dB. In the second experiment, we consider moving sources with lower angular velocities $\boldsymbol{\theta}_0 = [30^\circ, 50^\circ]$, $\boldsymbol{\theta}_1 = [0.06^\circ, -0.1^\circ]$. A sliding window of 25 snapshots is used in the LPA beamforming. The REM II is initialized by the LPA beamforming in the first scenario and ML method in the second one. To ensure the same data length in each time interval, we use additional $(W - 1)$ samples in the LPA beamforming processing.

The estimated trajectories presented in figs. 13 and 14 are very close to the true ones. The RMSEs of $\boldsymbol{\theta}_0$ and $\boldsymbol{\theta}_1$ corresponding to the first source are plotted in figs. 15 and 16. Using the initial value provided by LPA beamforming, RMSE associated with REM II changes slowly over the time. While estimates of $\boldsymbol{\theta}_0$ remains constant, the estimates of $\boldsymbol{\theta}_1$ become more accurate with increasing recursions. Also, we can observe that while LPA beamforming provides an overall better $\boldsymbol{\theta}_0$ estimates, and a better angular velocity estimates at beginning of the recursion, REM II improves $\boldsymbol{\theta}_1$ estimates with increasing time and has less fluctuations.

Compared with the Cramér-Rao bounds (CRB) [21] plotted in solid lines (—), one realizes that an REM II is certainly not efficient estimator. However, the ML approach suggested in [21], whose estimation accuracy is close to CRB, is a batch processing and requires a complicated multi-dimensional search procedure.

In the second experiment, REM II provides much more accurate estimates than LPA beamforming. Fig 17 shows that LPA beamforming even fails to follow the moving sources. We can observe in fig 19 that REM II has lower RMSE in both θ_0 and θ_1 estimation. Consequently, as shown in fig 20 the resulting DOA estimates are much better than LPA beamforming. In both experiments, the computational time needed for LPA beamforming is about 800 times as high as that required by REM II due to the two dimensional search procedure.

We conclude that REM I is suitable for tracking slowly time-varying DOA parameters, REM II performs well for both slowly and fast moving sources. Both procedures generate accurate estimates when there is no crossing point. When two source directions coincide with each other, the steering matrix $\mathbf{H}(\boldsymbol{\theta})$ becomes rank deficient. The signal waveform $\mathbf{s}(t)$ can not be determined properly. Consequently the DOA parameter can not be estimated accurately. In this case, regularization is needed [21]. Since REM II incorporates a linear polynomial model, it has a better tracking ability than REM I when this critical situation occurs. Compared to LPA beamforming, our method has a clear computational advantage. It provides comparable results with LPA beamforming in the fast moving sources case and outperforms LPA beamforming in the slow moving source case. In addition, recursive EM is applicable to both narrow band and broad band signals.

6 Conclusion

We addressed the problem of tracking multiple moving sources. Two recursive procedures are proposed to estimate the time-varying DOA parameter. We applied the recursive EM algorithm to a general case in which the motion of the sources is arbitrary and a specific case in which the motion of sources is described by a linear polynomial model. Because of the simple structure of the gain matrix, the suggested procedures are easy to implement. Furthermore, extension of our approaches to broadband signals is straightforward. Numerical experiments showed that our approaches provide excellent results in a slowly changing environment. When the DOA parameter changes fast or two source directions cross with each other, the procedure derived

for a linear polynomial model has a better performance than the general procedure. Important issues such as step size design and convergence analysis are still under investigation.

Acknowledgments

The authors thank the anonymous reviews for their constructive comments that significantly improved the manuscript and also thank Associate Editor J. C. Chen for coordinating a speedy review.

References

- [1] A. Benveniste, M. Métivier and P. Priouret, *Adaptive Algorithms and Stochastic Approximations*, Springer Verlag, 1990.
- [2] J. F. Böhme, “Array Processing”, *Advances in Spectrum Analysis and Array Processing*, pp. 1–63, Editor S. Haykin, Prentice Hall, Englewood Cliffs, N.J., 1991.
- [3] J. F. Böhme, “Statistical Array Signal Processing of Measured Sonar and Seismic Data”, *Proc. SPIE 2563 Advanced Signal Processing Algorithms*, pp. 2–20, San Diego, July 1995.
- [4] D. R. Brillinger, *Time Series: Data Analysis and Theory*, Holden-Day, 1981, San Francisco.
- [5] Erdinç Çekli and Hakan A. Çырpan, ”Unconditional Maximum Likelihood Approach for Localization of Near-Field Sources: Algorithm and Performance Analysis,” *AEÜ International Journal of Electronics and Communications*, Vol. 57, No. 1, pp. 9-15, 2003
- [6] P. J. Chung and J. F. Böhme, “Recursive EM and SAGE Algorithms”, *Proc. IEEE Workshop on Statistical Signal Processing*, pp. 540–542, Singapore, August, 2001.
- [7] P. J. Chung, “Fast Algorithms for Parameter Estimation of Sensor Array Signals”, Doctoral thesis, Dept. of Electrical Engineering and Information Sciences, Ruhr-Universität Bochum, Universitätsverlag Bochum, May, 2002.
- [8] P. J. Chung and J. F. Böhme, “DOA Estimation of Multiple Moving Sources Using Recursive EM Algorithms”, *Proc. Sensor Array and Multi-channel Signal Processing Workshop*, Washington DC, USA, August, 2002.

- [9] P. J. Chung, Johann F. Böhme: “Recursive EM and SAGE Algorithms with Application to DOA Estimation”, submitted to IEEE Transactions on Signal Processing, 2003.
- [10] P. J. Chung, J. F. Böhme: “Recursive EM Algorithm with Adaptive Step Size”, *Proc. The Seventh International Symposium on Signal Processing and Its Applications*, Paris, France, July 1–4, 2003.
- [11] A. P. Dempster and N. Laird and D. B. Rubin, ”Maximum Likelihood from Incomplete Data via the EM Algorithm”, *Journal of the Royal Statistical Society*, B39:1–38, 1977.
- [12] M. Feder and E. Weinstein, “Parameter estimation of Superimposed Signals Using the EM Algorithm” *IEEE Trans. on ASSP* , 36(4):477-489, April 1988.
- [13] L. Frenkel and M. Feder, “Recursive Expectation and Maximization (EM) Algorithms for Time-varying Parameters with Application to Multiple Target Tracking”, *IEEE Trans. Signal Processing*, 47(2):306–320, February 1999.
- [14] G. H. Golub and C. F. Van Loan, *Matrix Computations*, 3rd Edition, John Hopkins University Press, 1996.
- [15] D. Maiwald, “Breitbandverfahren zur Signalentdeckung und -ortung mit Sensorgruppen in Seismik- und Sonaranwendungen”, Doctoral thesis, Dept. of Electrical Engineering and Information Sciences, Ruhr-Universität Bochum , Shaker Verlag, Aachen, 1995.
- [16] Nihat Kabaoglu, Hakan A. Cirpan, Erdinc Cekli and Selcuk Paker, ”Deterministic Maximum Likelihood Approach for 3-D Near-Field Source Localization”, *AEÜ International Journal of Electronics and Communications*, Vol. 57, No. 5, pp. 345-350, 2003.
- [17] V. Katkovnik and A. B. Gershman, “ A Local Polynomial Approximation Based Beamforming for Source Localization and Tracking in Nonstationary Environments” *IEEE Signal Processing Letters*, 7(1):3-5, January 2000.
- [18] D. M. Titterington, “ Recursive Parameter Estimation using Incomplete Data” , *J. R. Statist. Soc. B*, 46(2):257–267, 1984.
- [19] D. M. Titterington and A. F. Smith and U. E. Makov “Statistical Analysis of Finite Mixture Distributions”, John Wiley & Sons, New York, 1985.

- [20] M. Wax and I. Ziskind, "Detection of the Number of Coherent Signals by the MDL Principle", *IEEE Trans. Acoust., Speech., Signal Processing*, 37(8):1190-1196, 1989.
- [21] T. Wigern and Eriksson, "Accuracy Aspects of DOA and Angular Velocity Estimation in Sensor Array Processing", *IEEE Signal Processing Letters*, 2(4), April 1995
- [22] B. Yang, "Projection Approximation Subspace Tracking", *IEEE Trans. Signal Processing*, 43(1):95-107, January 1995.
- [23] R. E. Zarnich and K. L. Bell and H. L. Van Trees, "A unified Method for Measurements and Tracking of Contacts From an Array of Sensors", *IEEE Trans. Signal Processing*, 49(12):2950-2961, December 2001.

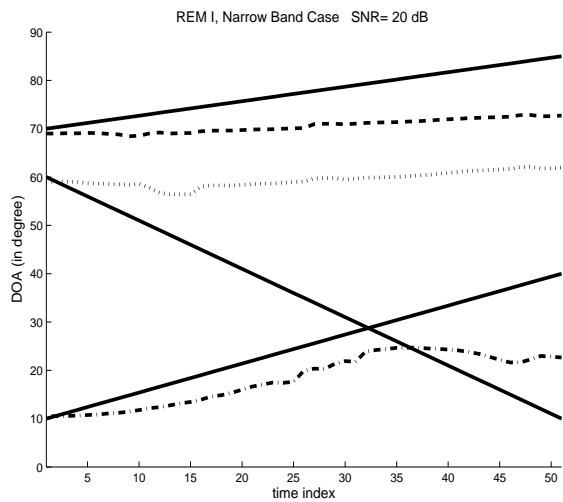


Figure 1: True trajectory (—) and estimated trajectory (---) by REM I. $\theta_0 = [10^\circ, 60^\circ, 66^\circ]$, $\theta_1 = [0.6^\circ, -1.0^\circ, 0.4^\circ]$.

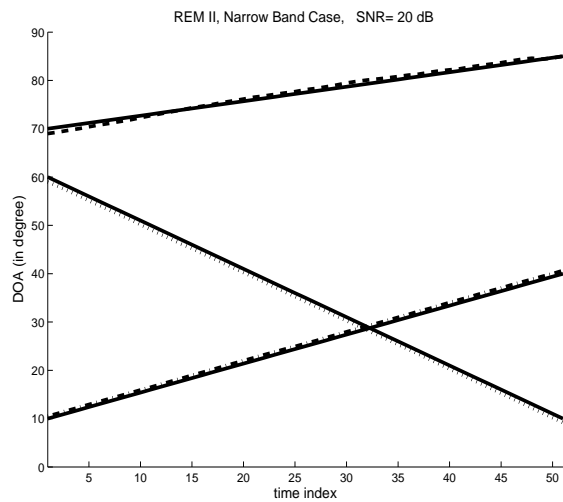


Figure 2: True trajectory (—) and estimated trajectory (---) by REM II.

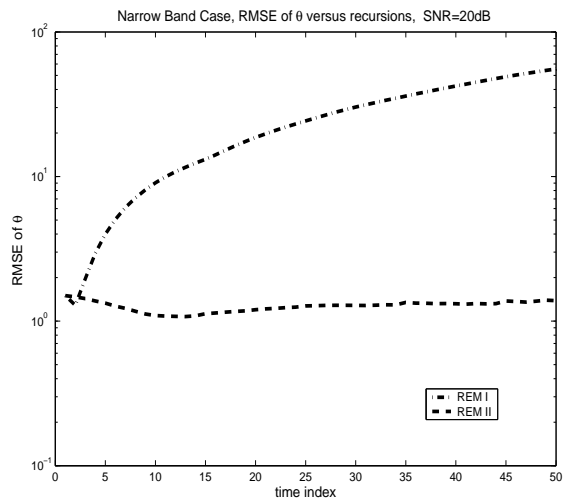


Figure 3: RMSE vs time. SNR=20 dB.

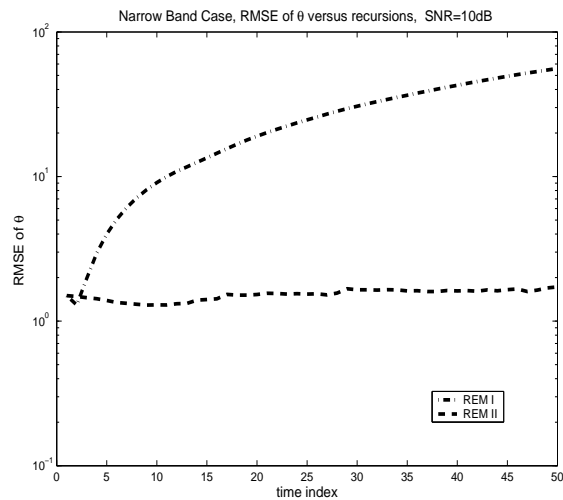


Figure 4: RMSE vs time. SNR=10 dB.

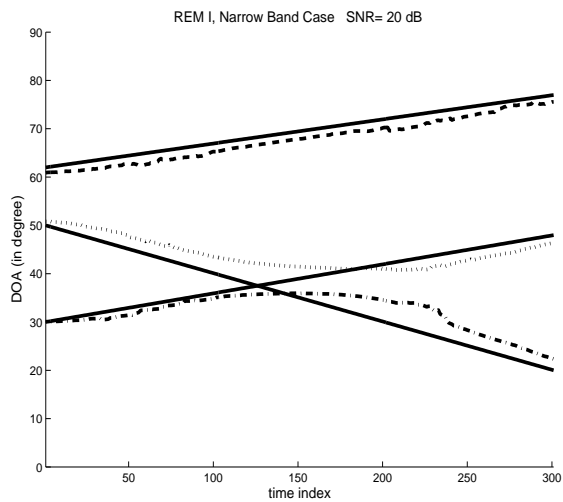


Figure 5: True trajectory (—) and estimated trajectory (---) by REM I. $\theta_0 = [30^\circ, 50^\circ, 62^\circ]$, $\theta_1 = [0.06^\circ, -0.1^\circ, 0.05^\circ]$.

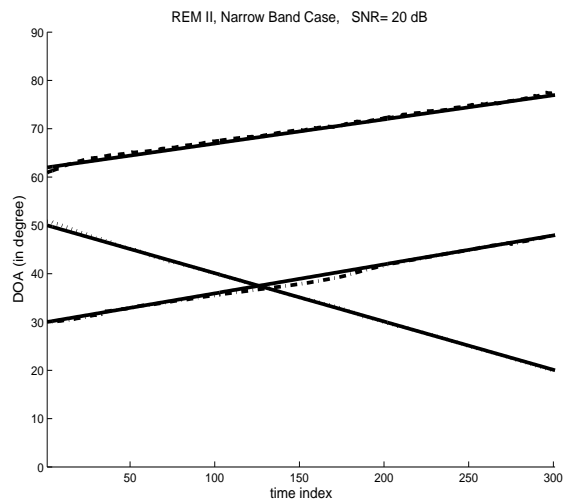


Figure 6: True trajectory (—) and estimated trajectory (---) by REM II.

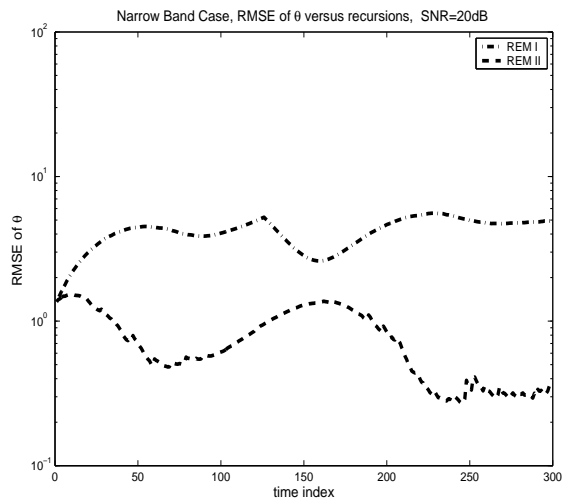


Figure 7: RMSE vs time. SNR=20 dB.

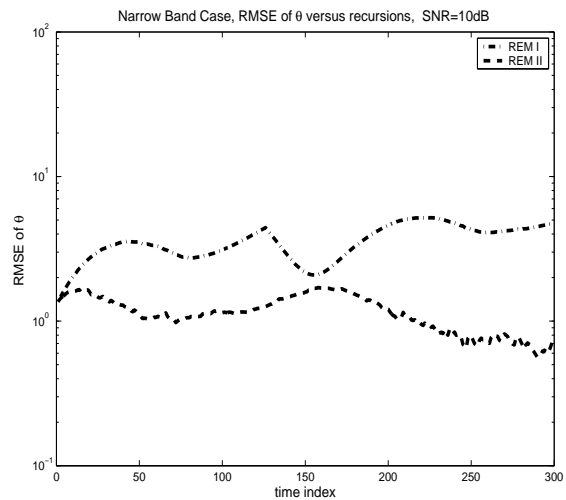


Figure 8: RMSE vs time. SNR=10 dB.

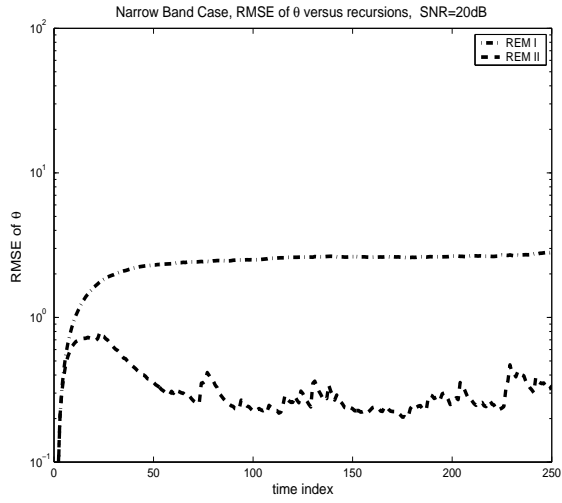


Figure 9: RMSE vs time. SNR=20 dB. $\theta_0 = [10^\circ, 30^\circ, 62^\circ]$, $\theta_1 = [0.08^\circ, 0.1^\circ, 0.06^\circ]$.

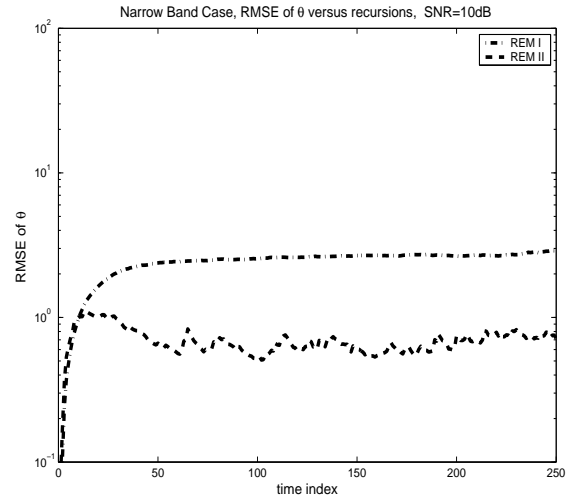


Figure 10: RMSE vs time. SNR=10 dB.

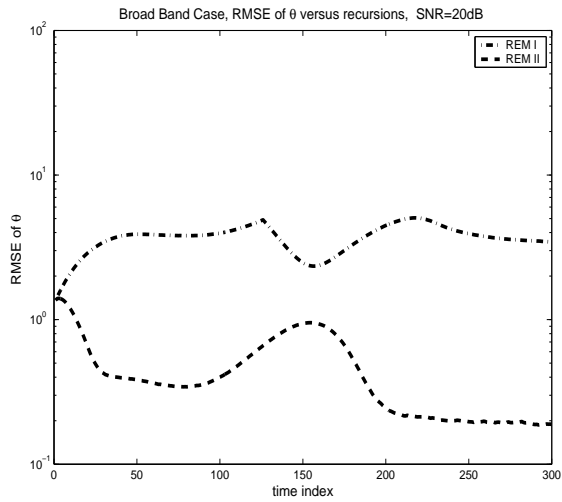


Figure 11: RMSE vs time. SNR=20 dB. $\theta_0 = [30^\circ, 50^\circ, 62^\circ]$, $\theta_1 = [0.06^\circ, -0.1^\circ, 0.05^\circ]$. Number of frequency bins = 3.

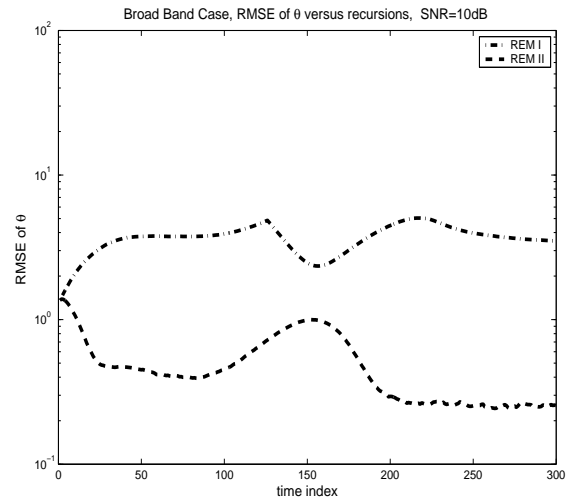


Figure 12: RMSE vs time. SNR=10 dB.

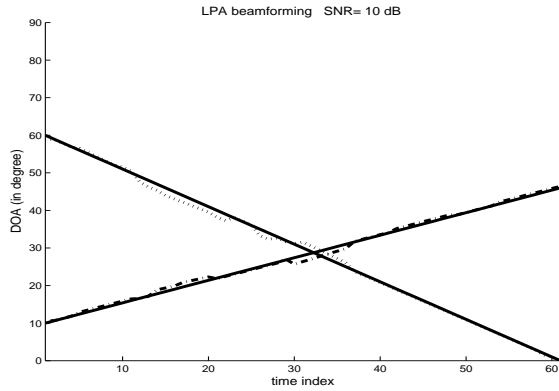


Figure 13: True trajectory (—) and estimated trajectory (---) by LPA Beamforming. $\theta_0 = [10^\circ, 60^\circ]$, $\theta_1 = [0.6^\circ, -1.0^\circ]$.

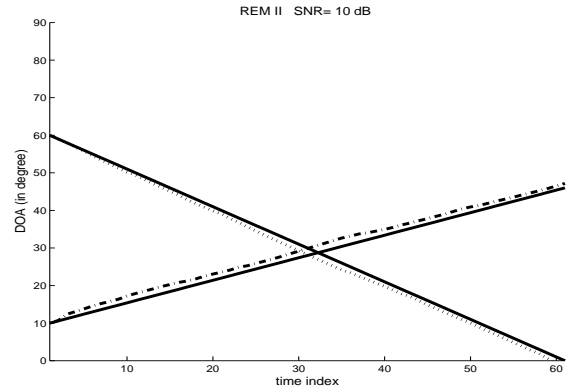


Figure 14: True trajectory (—) and estimated trajectory (---) by REM II.

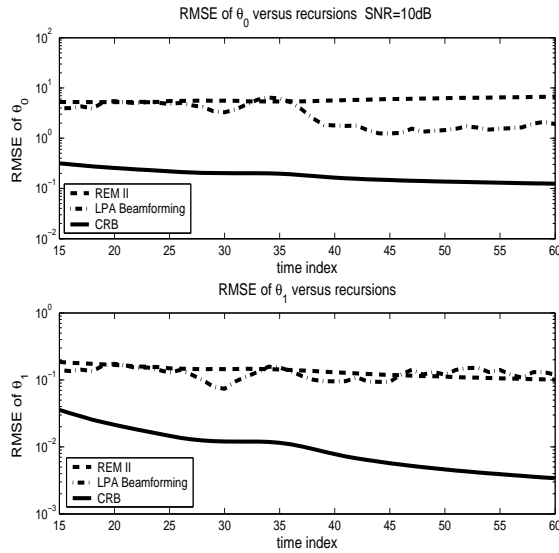


Figure 15: Upper: RMSE of θ_0 the 1st Source vs time. Lower: RMSE of θ_1 vs time. SNR= 10dB.

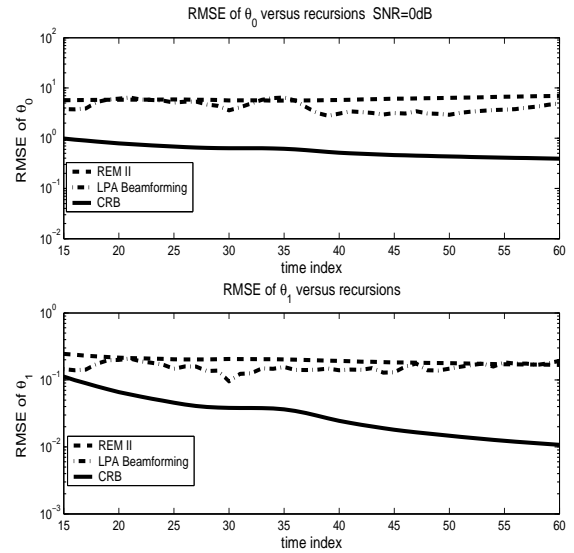


Figure 16: Upper: RMSE of θ_0 the 1st Source vs time. Lower: RMSE of θ_1 vs time. SNR= 0dB.

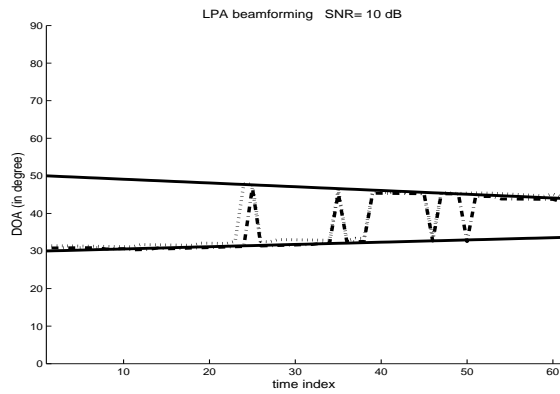


Figure 17: True trajectory (—) and estimated trajectory (---) by LPA Bemaforming. $\theta_0 = [30^\circ, 50^\circ]$, $\theta_1 = [0.06^\circ, -0.1^\circ]$.

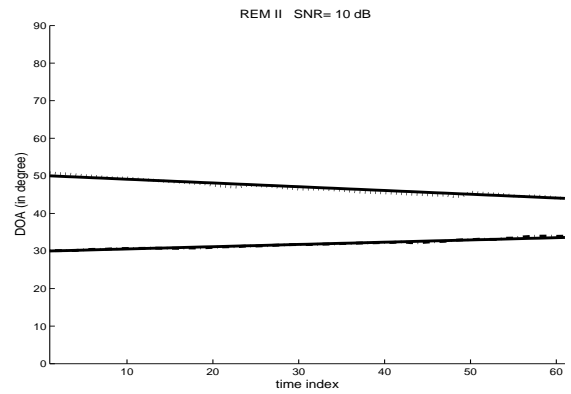


Figure 18: True trajectory (—) and estimated trajectory (---) by REM II.

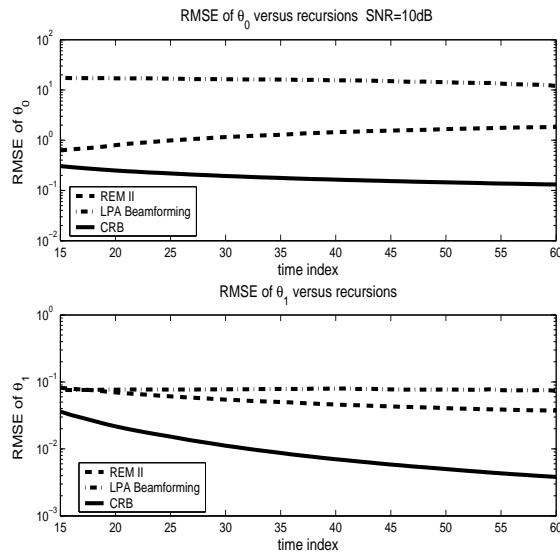


Figure 19: Upper: RMSE of θ_0 the 1st Source vs time. Lower: RMSE of θ_1 vs time. SNR= 10dB.

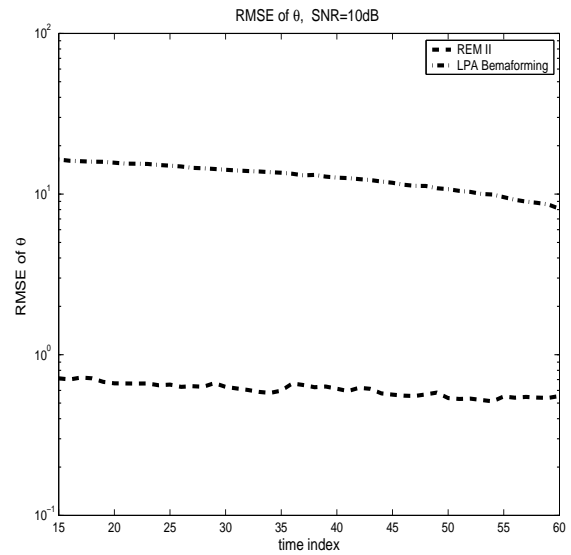


Figure 20: RMSE of θ vs time.